Journal of Alloys and Compounds 641 (2015) 22–29

Contents lists available at ScienceDirect

Journal of Alloys and Compounds

journal homepage: www.elsevier.com/locate/jalcom

The effect of Nb–B inoculation on binary hypereutectic and near-eutectic LM13 Al–Si cast alloys

M. Nowak, L. Bolzoni *, N. Hari Babu

Brunel University London, Institute of Materials and Manufacturing, Uxbridge, Middlesex UB8 3PH, UK

ARTICLE INFO

Article history:
Received 16 December 2014
Received in revised form 26 March 2015
Accepted 7 April 2015
Available online 11 April 2015

Keywords:
Metals and alloys
Microstructure
Heterogeneous nucleation
Nb–B inoculation

ABSTRACT

Hyper-eutectic Al–Si alloys are used for wear-resistant components, such as pistons, because their microstructure is composed by ductile aluminium dendrites and hard primary silicon particles. In this study the effect of Nb–B inoculation on the microstructural features of binary hyper-eutectic and near-eutectic LM13 Al–Si alloys is assessed. It is found that the inoculation with Nb-based compounds (i.e. NbB_2 and Al_3Nb) leads to the refinement of the microstructural features (i.e. finer and more homogeneous distribution of the eutectic phase as well as smaller primary Si particles as secondary effects). The study also demonstrates that the addition of Nb–B inoculants do not interfere with additions of strontium (used to modify the morphology of the eutectic phase) or phosphorous (added to nucleate primary Si particles).

1. Introduction

Aluminium alloys are conventionally divided into wrought and cast depending on whether the primary processing is carried out by means of a deformation method or not [1]. The principal alloying element of aluminium cast alloys is silicon because it confers sufficient fluidity to the molten metal to satisfactorily fill die cavities as well as obtain good surface finishing. The Al–Si binary phase diagram is the typical eutectic diagram for a two-component mixture whose eutectic point is located at a content of 12.6 wt.% of silicon and a temperature of 577 °C [2]. Because of this aspect, Al–Si cast alloys, whose silicon content is generally higher than 4 wt.%, are classified into three main groups depending on the amount of silicon present: hypo-eutectic (4–11 wt.%), near-eutectic (11–13 wt.%) and hyper-eutectic (>13 wt.%) [3]. Depending on the type of alloy there are differences in the relative amount and morphology of the microconstituents of Al–Si alloys although they are exactly the same: primary α-Al dendrites (i.e. ductile and soft solid solution of silicon in aluminium), eutectic phase (i.e. brittle and hard Al–Si intermetallic particles) and primary silicon particles. More in detail, the eutectic phase present in Al–Si cast alloy is commonly characterised by a 3D planar (lath) or 2D acicular morphology [4] which can be useful in application where high wear resistance is required but it is detrimental for the ductility of the material. The morphology of this eutectic phase can be easily changed to fibrous by the addition of very small quantity (ppm) of calcium, sodium and strontium; a process known as modification [5–9]. On the base of the stable binary phase diagram, primary silicon particles should be present as microstructural features exclusively in hyper-eutectic Al–Si alloy. Nevertheless, because the solidification of the alloys does not take place under equilibrium conditions and there is partitioning of the solute in the solidification front, primary silicon particles are generally found also in Al–Si alloys with silicon content lower than the eutectic composition. As for the intermetallic phase, these brittle and hard primary silicon particles can be useful for structural components of the engine block [10]. For that, in the case of hyper-eutectic Al–Si alloys, few ppm of phosphorus are conventionally added in order to decrease the final size and increase the total number of primary Si particles that form upon solidification [11]. Depending on the nature of the material, Al–Si cast alloys find different applications in the automotive industry such as wheels (hypo-eutectic), engine blocks (near-eutectic) and pistons (hyper-eutectic). It is well known that the processability and mechanical performances of aluminium alloys can be improved by means of grain refinement. Actually, this is quite well-established industrial practise for wrought aluminium alloys, where the refinement is done by means of Al–Ti–B master alloys [12–15]. The drawback of using these commercial master alloys on Al–Si cast alloys is the formation of titanium silicides which prevents the effective grain refinement of the alloy, a phenomenon known as poisoning [16–21]. We recently published a work about the development of an efficient Nb–B grain refiner for Al–Si where it was found that Nb–B inoculation leads to the refinement of both primary α-Al dendrites and eutectic phase of hypo-eutectic Al–Si alloys [22–26]. The aim

* Corresponding author. Tel.: +44 1895 267202; fax: +44 1895 269758.
E-mail address: leandro.bolzoni@brunel.ac.uk (L. Bolzoni).

http://dx.doi.org/10.1016/j.jallcom.2015.04.053
0925-8388/

of this work is to study the effect of Nb–B inoculation on the microstructural features of near-eutectic and hyper-eutectic Al–Si alloys in order to better understand the full grain refining potency of Nb–B based grain refiners. In grain refinement work, it is very common to carry out the comparison of the performances of new grain refiners with that of the well-established Al–5Ti–1B master alloy. Nonetheless, in this case the authors did not consider any commercial Al–Ti–B refiners because they are characterised by poisoning and, in the best knowledge of the authors, do not have any effect at all on any other microstructural feature (especially primary Si particles) than the primary α-Al dendritic grains.

2. Experimental procedure

The investigation about the effect of Nb–B inoculation in commercial near-eutectic and hyper-eutectic Al–Si alloys was divided into two parts. In the first set of experiments binary lab-produced hyper-eutectic Al–*x*Si alloys, where $x = 14–27$ wt.%, were tested whilst in the second set of experiments the commercial Al–Si alloy LM13 was considered. The chemical composition of the raw material used is shown in Table 1.

2.1. Binary hyper-eutectic Al–xSi alloys

Binary hyper-eutectic Al–*x*Si alloys were prepared by mixing the appropriate amount of commercially pure Al with the Al–50Si master alloy. The chemical compositions studied were: Al–14Si, Al–16Si, Al–18Si, Al–20Si and Al–27Si. Specifically, batches of 5 kg of each Al–*x*Si alloy were produced by melting the raw materials (chemical composition specified in Table 1) into clay-bonded graphite crucibles at 800 °C during 1 h and then cast into rectangular ingots. The chemical composition of the cast binary hyper-eutectic Al–*x*Si was checked by means of optical emission spectroscopy (OES). It is worth mentioning that the variation of the chemical composition was lower than 0.1 wt.% for each of the binary Al–*x*Si alloys. For the inoculation experiments, the Al–*x*Si alloys were melted in an electric resistance furnace at 800 °C after which Nb–B inoculants were added (targeted, 0.1 wt.% of Nb and B) [22–24]. Nb was added in the form of powder (Nb > 99.8%, particle size lower than 45 μm) and boron by potassium tetrafluoroborate flux (KBF_4 > 98%). Therefore, the actual Nb and B contents are expected to be somewhat lower due to the oxidation of the Nb powder particle and the poor recovery, at lab scale, of B from the KBF_4 flux. After, at least, 1 h of dissolution time, both reference and Nb–B inoculated samples were left to cool down to 700 °C and cast under similar conditions using a preheated steel mould (cooling rate ~1 °C/s). Samples were prepared for metallographic analysis using SiC grinding papers and OPS polishing solution. Grain size of the materials was determined as specified in the ASTM: E112 standard.

2.2. Commercial near-eutectic LM13 alloy

This commercially available and industrially employed near-eutectic alloy (whose composition was reported in Table 1) was used because upon solidification it will be characterised by the three main microstructural features of the binary Al–Si phase diagram and it gives a comprehensive idea of the effect of Nb–B inoculation on them. The LM13 alloy is conventionally employed to fabricate engine components like pistons for gasoline and diesel motors and, therefore, the material is cyclically stressed both mechanically and thermally. The properties required for this material are high fatigue resistance and lifetime as well as good wear resistance which are achieved in the hyper-eutectic Al–Si alloys due to the presence of coarse, angular primary silicon particles embedded within the soft and ductile aluminium dendrites [27]. As already indicated, it is a common practise to modify the morphology of the eutectic phase from planar to fibrous by means of strontium [6] and/or decrease the final size and increase the total number of primary silicon particles that form during solidification using phosphorous [11]. In the view of this fact, experiments were done considering the effect of the addition of Nb–B inoculants on the LM13 simultaneously without and with the addition of 200 ppm of strontium or 100 ppm of phosphorus. In particular, the materials cast were: reference alloy (LM13), Nb–B inoculated LM13 alloy (LM13 + Nb–B), strontium-modified reference alloy (LM13 + Sr), Nb–B inoculated strontium-modified LM13 alloy (LM13 + Nb–B + Sr), phosphorous-modified reference alloy (LM13 + P) and phosphorous-modified Nb–B inoculated LM 13 alloy (LM13 + Nb–B + P). The same experimental procedure (i.e. melting parameters, casting conditions, samples preparation and microstructural analysis) that was used for the binary hyper-eutectic alloys was used for the commercial LM13 alloy.

Table 1
Chemical composition of the materials used.

Element (wt.%)	Material		
	CP-Al	Al–50Si	LM13
Al	>99.5	50	Balance
Si	0.02	50	10.5–13.0
Mg	–	–	0.8–1.5
Fe	0.08	–	1.0
Cu	–	–	0.7–1.5
Mn	0.01	–	0.5
Ni	–	–	1.5
Zn	0.02	–	0.1
Ti	0.06	–	0.1

3. Results and discussion

3.1. Effect of Nb–B inoculation on the microstructural features of binary hyper-eutectic Al–xSi alloys

Fig. 1 shows the microstructure of the binary Al–14Si alloy without and with the addition of Nb–B inoculants where the presence of primary α-Al dendrites branches have been highlighted. It is important to remark that although hyper-eutectic Al alloys were investigated, primary α-Al grains were detected in some of the alloys investigated, especially in those with chemical composition near the eutectic point such as in the case of the Al–14Si alloy. This is because during solidification the melt becomes enriched in solute, especially Si, and the process does not occur under conditions of equilibrium. Moreover, the addition of ternary alloying elements (i.e. Nb and/or B) and/or modifiers (i.e. Sr and P) as well as impurities (see Table 1) shifts the eutectic point and displaces

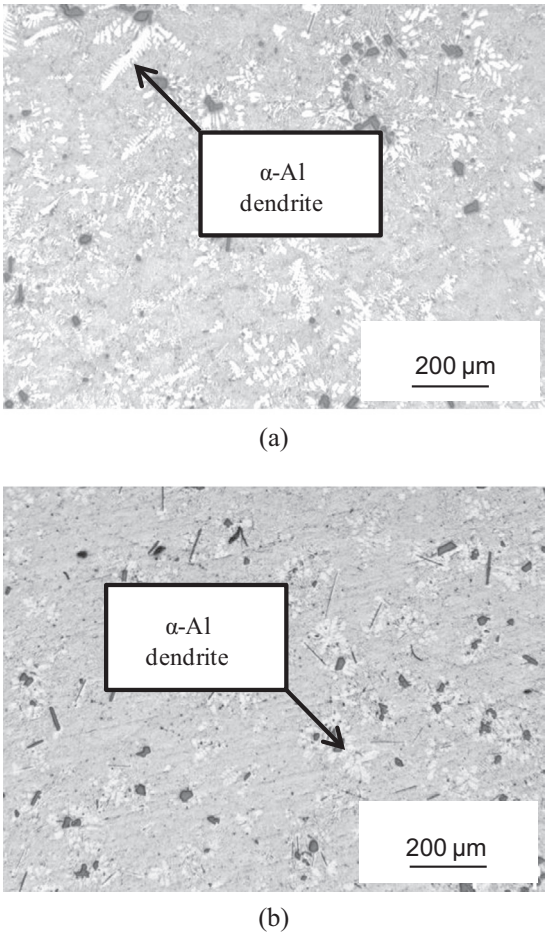

Fig. 1. Micrographs of the Al–14Si alloy without (a) and with (b) Nb–B inoculation.

the eutectic temperature, normally to higher Si percentages and lower eutectic temperatures [28,29], although their contribution is relatively weak in comparison to the effect of non-equilibrium solidification.

By comparing the micrographs of the Al–14Si alloy without and with the addition of Nb–B inoculants, it is evident that the size of the few primary α-Al dendrites that can be distinguished in the microstructure is finer in the Nb–B inoculated material. This fact confirms the potency of the Nb-based compounds for the refinement of primary α-Al dendrites [30] and indicates that Nb–B inoculation is also effective in hyper-eutectic Al–Si alloys. In a previous study about the characterisation of the compounds that form upon the mixing of Nb powder and KBF_4, we demonstrated the formation of NbB_2 and Al_3Nb compounds which are responsible for the refinement of Al–Si alloys [22–24]. Specifically, NbB_2 and Al_3Nb are characterised by hexagonal (a = 3.102 Å, c = 3.285 Å) and tetragonal (a = 3.848 Å, c = 8.615 Å) crystal structure and their lattice mismatch along low-index planes is 30.6% and 4.2% respectively [1]. As in the case of Al–Ti–B master alloy where it is believed that a transition layer of Al_3Ti is formed onto the surface of TiB_2 particle because Al_3Ti has much higher favourable lattice match [31], the same mechanism can be applied in the case of Nb-based inoculants. As previously mentioned, the other two important microstructural features of the near-eutectic and hyper-eutectic Al–Si alloys are the intermetallic phase and the primary silicon particles. Figs. 2 and 3 summarise the effect of the Nb–B refiner on the binary hyper-eutectic Al–xSi alloy (where x = 14–27 wt.%) for the eutectic phase and the primary silicon particles, respectively. It is worth mentioning that the size of the eutectic phase refers to the length of the needle present on the cross-section of the polished samples.

By comparing the microstructures of the Al–Si alloys presented in Fig. 2, it can be noticed that after Nb–B inoculation the eutectic phase is finer and still characterised by needle shape. Moreover, it can be seen that the eutectic phase becomes coarser with the increment of the Si content independently of the addition of any refiner but it is always finer when the melt is treated with Nb–B inoculants. More in detail, from Fig. 2(g), the distribution of the eutectic phase of the binary Al–18Si alloy is quite wide and ranges approximately from 3 μm to 10 μm and most of the data are concentrated around 4 μm. The addition of the Nb–B refiner shifts the mean size towards lower values (i.e. 2–4 μm) and the great majority of the eutectic phase has a size of about 2 μm. Statistical analysis of the distribution of the data (a Gaussian distribution was assumed since nucleation is a pure stochastic process) confirmed the shorter length of the eutectic lamellae after Nb–B inoculation (2.1 ± 0.04 μm) with respect to the reference material (3.6 ± 1.4 μm). The refinement of the eutectic phase is thought to be by heterogeneous nucleation from the Nb-based compounds due to the low lattice mismatch with the α-Al phase. Specifically, it was demonstrated that, at the beginning of solidification, Nb–B inoculants promote the nucleation of a large number of Al grains. With the progression of solidification, the Al–Si eutectic phase starts to nucleate due to the enrichment in Si of the remaining melt and it does nucleate between the braches of Al dendrites. The large number of Al grains, whose lattice parameters do not differ significantly from those of the eutectic phase, and the more homogeneous distribution of Si in the liquid pools, consequently, induce the formation of a much greater number of eutectic particles. The refinement of the eutectic phase, therefore, is a consequence of the refinement of the dendritic Al grains as the lattice parameters difference (Si crystallizes into tetrahedral structure, a = 5.431 Å) does not seem to be favourable for its nucleation.

From analysis of the micrographs of the binary Al–Si alloys studied (Fig. 3), it is not easy to discern a clear effect of Nb–B inoculation on the primary silicon particles. The polyhedral-shaped particles present in the Al–16Si alloy seems smaller, the length of the flake-like particles in the microstructure of the Al–18Si alloy is finer and the formation of coarse primary silicon particles characterised by fish-bone, flake-like and star-like shapes particles, typical of very high silicon content Al–Si alloys, is somewhat hindered. From the results of the statistical analysis of the total number of particles present in relation to their size for the Al–16Si alloy (Fig. 3(g)) it is demonstrated quantitatively that the addition of the Nb–B refiner shifts the distribution of the size of primary silicon particles towards the left (i.e. smaller size). Moreover, it can be seen that the total number of finer Si particles is much greater and approximately 70% of the particles are finer than 40 μm. In particular, the experimental data were fitted with a Gaussian distribution (stochastic process) obtaining mean primary silicon particle size of 36.6 ± 4.4 μm and 13.9 ± 9.1 μm for the reference and the Nb–B inoculated binary Al–16Si alloy. As in the case of the eutectic phase, the effect of Nb-based intermetallics on the size and distribution of primary silicon particles is a consequence of the enhanced nucleation of the dendritic Al grains. In Fig. 3(h) the expected trends for the number and size of primary silicon particles for the reference and the Nb–B inoculated alloy were superimposed on the binary Al–Si phase diagram. As it can be seen, the total number of primary silicon particles, which start to form around the eutectic composition, increases along with the increment of the Si content (in this study up to 27 wt.% of Si). In the case of the employment of Nb–B inoculants, which are actually refining the dendritic α-Al grains, a greater number of primary silicon particles are formed due to the more uniform distribution of the reject solute in the solidification front and the smaller solidification pools remaining in between the dendritic arms. Nevertheless, this secondary effect fades away with the increment of the Si content. In general, the size and aspect ratio of the primary silicon particles is found to increase with the increment of the Si content where the enhancement of the nucleation of the dendritic grains through the addition of Nb-based intermetallics permits finer primary silicon particles once again as a consequence of the more homogenous distribution of the alloying element.

3.2. Effect of Nb–B inoculation on the microstructural features of untreated/modified commercial hyper-eutectic Al–Si alloys (LM13)

Fig. 4 shows representative examples of the microstructure of the LM13 alloy without and with the addition Nb–B inoculation on top of which the effect of the modification of the morphology of the eutectic Si by means of Sr was considered.

From the micrograph of the LM13 alloy shown in Fig. 4(a) and (b), it can be seen that the reference material is characterised by quite coarse primary α-Al dendrites, whose size ranges between 2000 and 2500 μm, relatively coarse planar Al–Si eutectic phase and iron-based intermetallics. Specifically, the common script-like α-phase identified as Al_8Fe_2Si, the plate-like β-phase known as Al_5FeSi, the script-like π-phase known as $Al_8FeMg_3Si_6$ and the blocky-like α-phase ($Al_{15}(Fe,Mn)_3Si_2$) are present [32]. The addition of Nb–B inoculants leads to the refinement of the size of the primary α-Al dendrites down to 500–1000 μm (Fig. 4(c)) and to a variation of the eutectic and intermetallic phases. After Nb–B inoculation (Fig. 4(d)) these secondary phases are expected to be slightly finer and more uniformly distributed throughout the microstructure as found during the study of binary hyper-eutectic alloys. The refining of the secondary Al–Si eutectic and Fe-based intermetallic phases is a consequence of the presence of a much greater number of α-Al grains which leads to a more homogeneous distribution of the rejected solute elements in the solidification front and pools. The modification of the reference LM13 alloy by means of the addition of strontium is very effective because the morphology of the eutectic Si phase is switched to

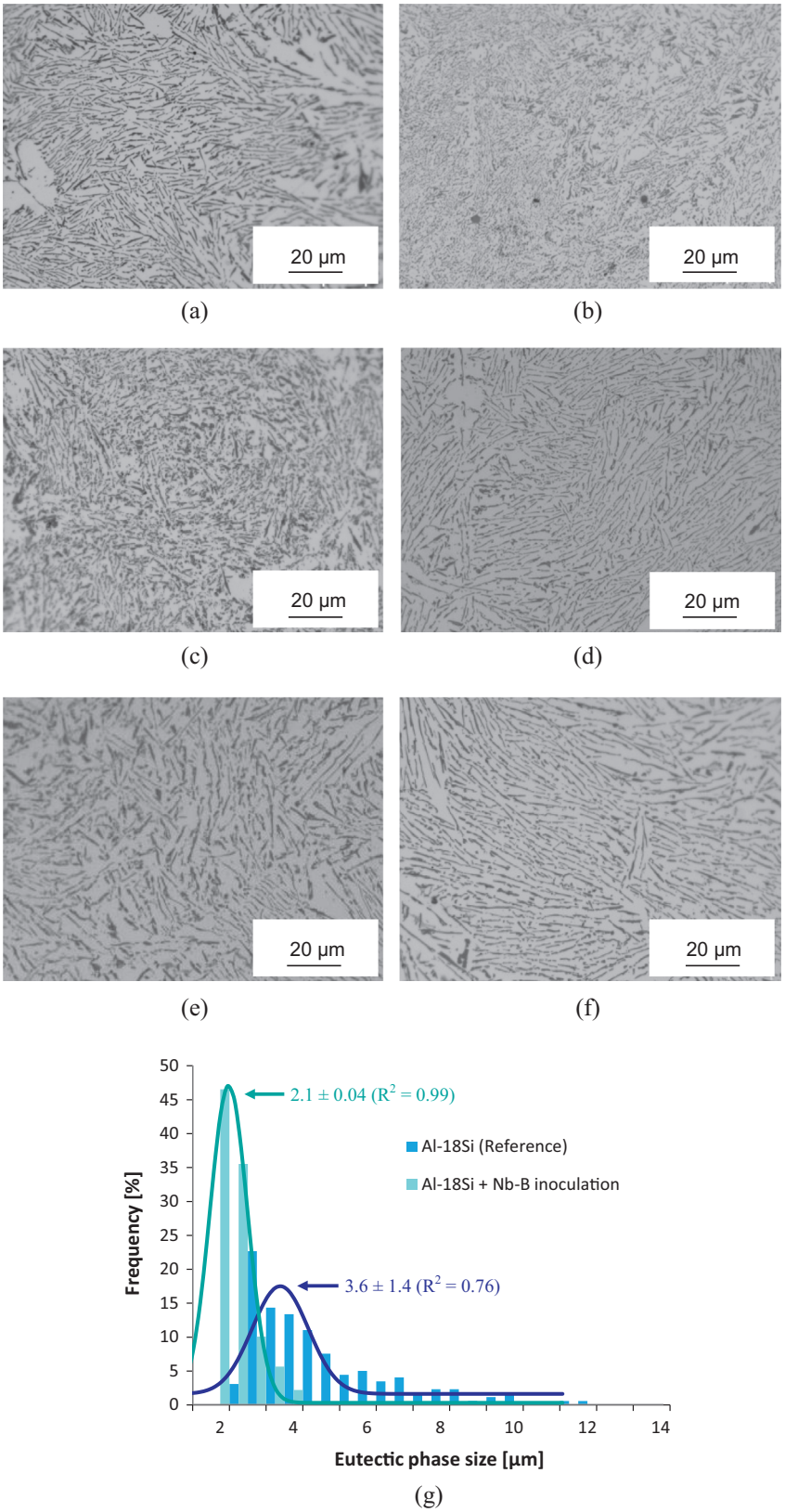

Fig. 2. Representative micrographs of the eutectic phase of: (a) Al–16Si, (b) Al–16Si + Nb–B inoculation, (c) Al–18Si, (d) Al–18Si + Nb–B inoculation, (e) Al–27Si and (f) Al–27Si + Nb–B inoculation; and (g) statistical distribution of the eutectic phase size for the Al–18Si alloy.

fibrous (Fig. 4(e) and (f)). Nevertheless, the distribution of this eutectic phase is still rather heterogeneous because it is mainly confined in between the secondary arms of coarse primary dendritic grains. The addition of 200 ppm of strontium together with Nb–B inoculants (Fig. 4(g) and (h)) does not seem to affect the efficiency of the refinement of the primary α-Al dendrites,

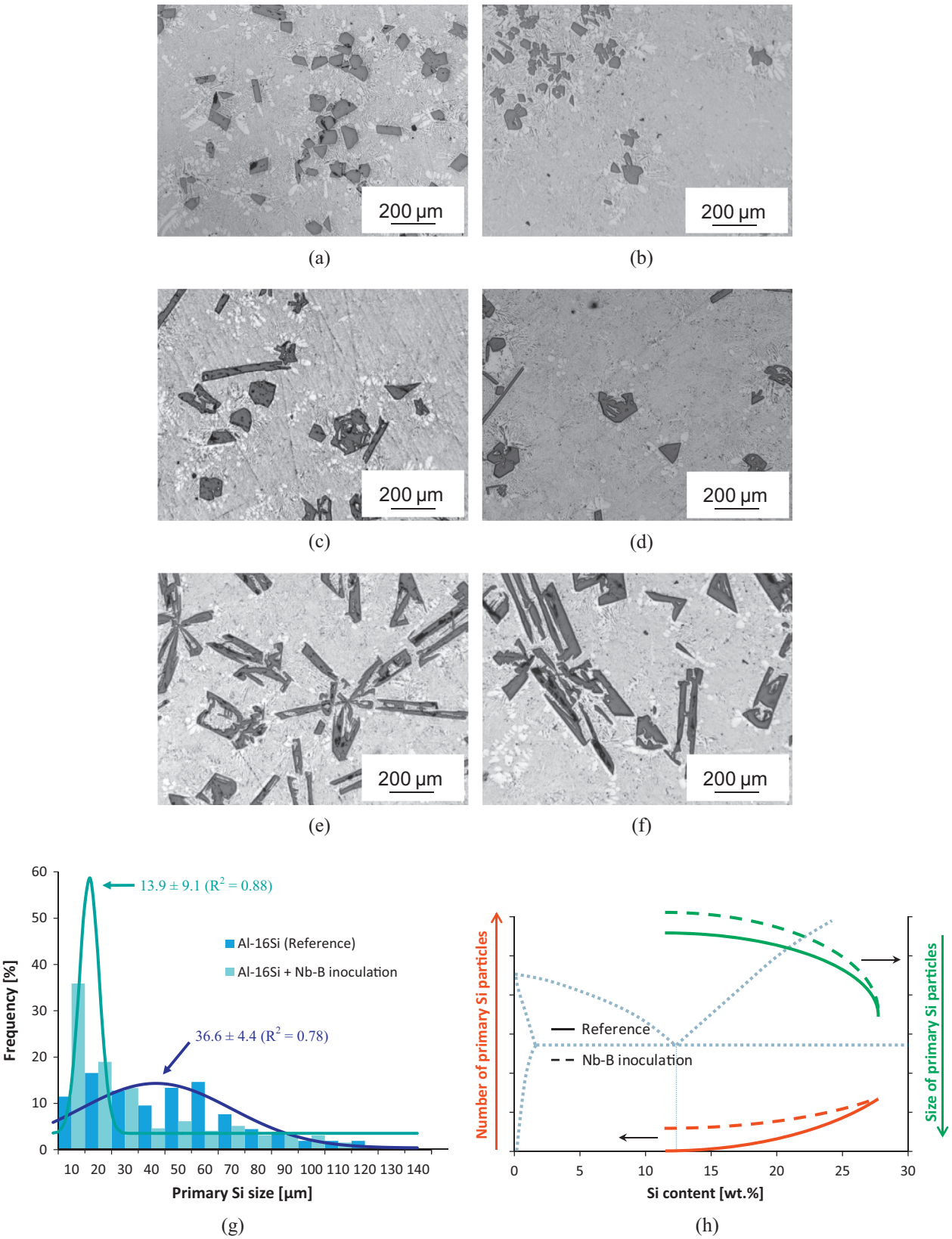

Fig. 3. Representative micrographs of the primary Si particles of: (a) Al–16Si, (b) Al–16Si + Nb–B inoculation, (c) Al–18Si, (d) Al–18Si + Nb–B inoculation, (e) Al–27Si and (f) Al–27Si + Nb–B inoculation, (g) statistical distribution of the primary silicon particles size for the Al–16Si alloy and (h) expected variation of the number and size of the primary silicon particles.

because their size is comparable to those found after the sole addition Nb–B inoculants (Fig. 4(c)). Furthermore, no reacted compounds based on the interaction between niobium, boron and strontium were found.

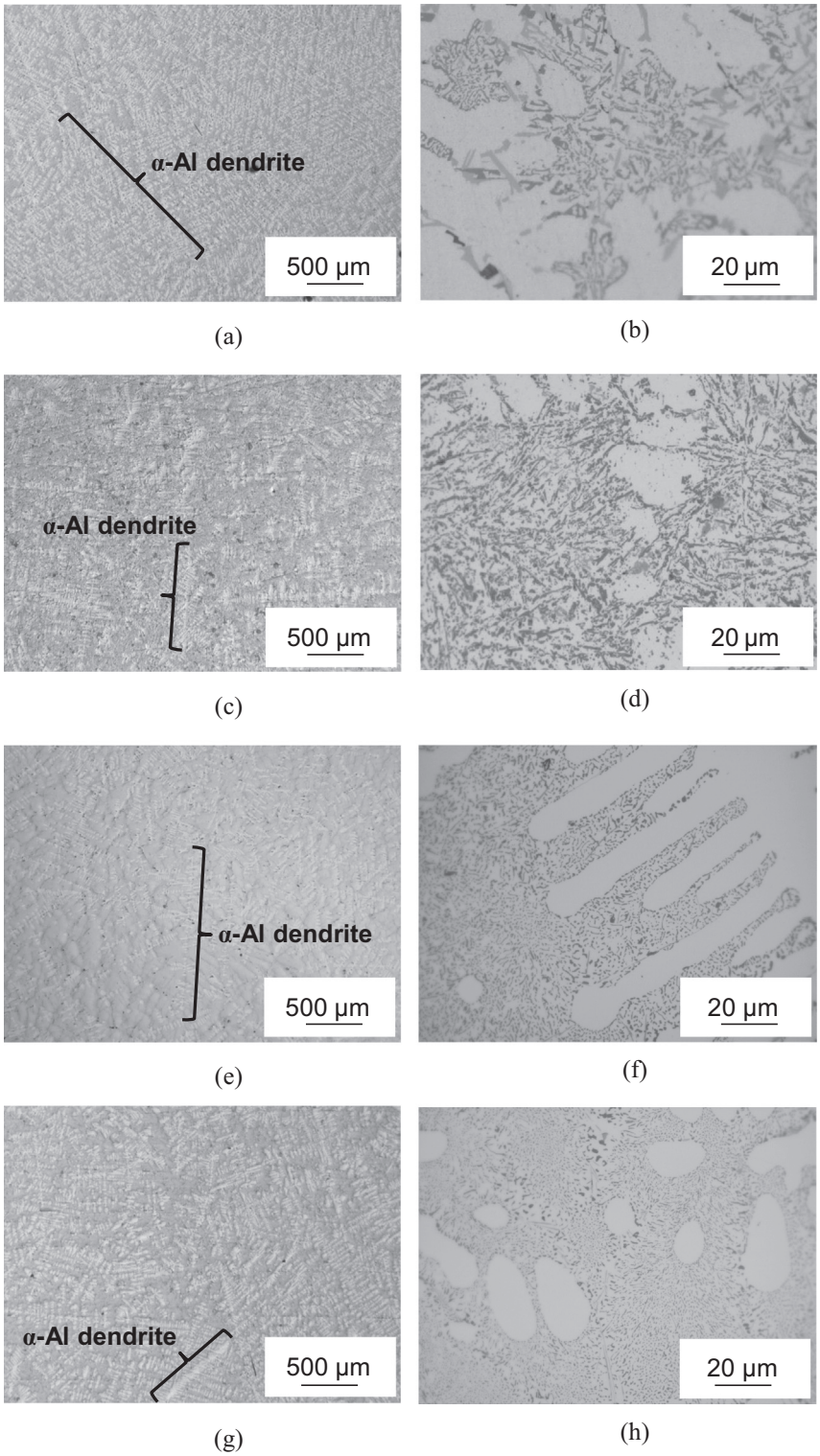

Fig. 4. Microstructural analysis of the LM13 alloy: (a) reference (primary α-Al dendrite grain size), (b) reference (eutectic phase), (c) LM13 + Nb–B inoculation (primary α-Al dendrite grain size), (d) LM13 + Nb–B inoculation (eutectic phase), (e) reference + strontium (primary α-Al dendrite grain size), (f) reference + strontium (eutectic phase), (g) LM13 + Nb–B inoculation + strontium (primary α-Al dendrite grain size) and (h) LM13 + Nb–B inoculation + strontium (eutectic phase).

Fig. 5 reports the micrographs of the LM13 alloy without and with the addition of Nb–B inoculants plus the addition of phosphorus for the promotion of the nucleation of primary silicon particles. It is worth recalling that these experiments were done using the same processing conditions of those whose results were discussed in Fig. 4.

From the analysis of the micrographs displayed in Fig. 5(a) and (b), it can be seen that the addition of phosphorus to the LM13 reference alloy fulfilled its purpose completely because many fine (~20–40 μm) primary silicon particles were nucleated during the solidification of this near-eutectic alloy with respect to the reference material without phosphorous addition

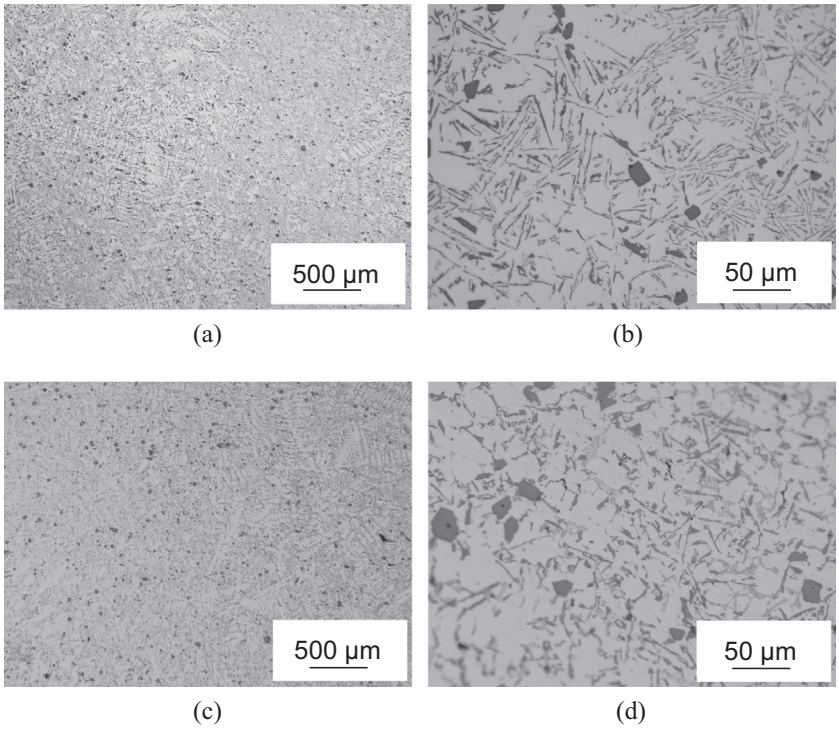

Fig. 5. Micrographs of the LM13 alloy: (a) reference + phosphorous (primary α-Al dendrite grain size), (b) reference + phosphorous (eutectic phase), (c) LM13 + Nb–B inoculation + phosphorous (primary α-Al dendrite grain size) and (d) LM13 + Nb–B inoculation + phosphorous (eutectic phase).

(Fig. 4(a) and (b)). No significant changes on the other two microstructural features (i.e. primary α-Al dendritic grains and eutectic phase) could be highlighted and this is expected because the only effect of phosphorous on Al–Si cast alloys is the to promote the formation/refinement of primary silicon particles in near-eutectic or hyper-eutectic Al–Si alloys, respectively. Concerning the combined addition of Nb–B inoculants and phosphorous, it can be seen in Fig. 5(c) and (d) that the size of the primary α-Al grains is comparable to that shown in Fig. 4(c) and (d) and finer with respect to the reference LM13 alloy (Fig. 4) confirming the enhancement of the heterogeneous nucleation of α-Al via the addition of Nb-based intermetallics. Moreover, because of the presence of phosphorus many primary silicon particles (whose size and distribution are comparable to those of the reference alloy inoculated with phosphorous) are embedded in the microstructure. From this it can be evinced that the effect of phosphorous and Nb–B inoculation on the microstructural features of the near-eutectic Al–Si alloys are not altered or compromised because they do not interact between each other.

4. Conclusions

From this study about the effect of Nb–B inoculation on near-eutectic and hyper-eutectic Al–Si alloys, it can be concluded that the nucleation of primary Al α-grains is highly promoted, the aluminium–silicon eutectic phase is significantly refined, the average size of the primary silicon particles is reduced and their total number is lowered. Nb-based compounds promote the heterogeneous nucleation of a significant number of primary α-Al dendrites and/or eutectic phase due to the low lattice mismatch. As a consequence of the more uniform distribution of the solute elements, and in particular silicon atoms, in the solidification front and pools, an enhancement (normally refinement) of the other microstructural features, whether they are secondary intermetallics phases or primary silicon particles, is obtained. Nevertheless, it is envisioned that this secondary effect fades away with the increment of the silicon content of the hyper-eutectic Al–Si cast alloys. Finally, the addition of Nb–B inoculants starting from powders does not lead to any poisoning effect and does not seem to prevent the modification of the morphology of the eutectic phase by strontium and/or the nucleation of primary Si particles by phosphorus.

Acknowledgements

The support from EP/J013749/1 Project and EP/K031422/1 Projects as well as TSB/101177 Project of the Engineering and Physical Sciences Research Council (EPSRC) and the Technology Strategy Board (TSB), respectively, is acknowledged.

References

[1] G.E. Totten, D. Scott Mac Kenzie, Handbook of Aluminium Vol. 2: Alloy Production and Materials Manufacturing, Marcel Dekker Inc., New York, Basel, 2003.
[2] ASM International, ASM Handbook Volume 03: Alloy Phase Diagrams, ASM International, Ohio, 1992.
[3] I.J. Polmear, Light Alloys. From Traditional Alloys to Nanocrystals, fourth ed., Butterworth-Heinemann, UK, 2006.
[4] A. Mazahery, M.O. Shabani, JOM 66 (2014) 726–738.
[5] S.-Z. Lu, A. Hellawell, J. Cryst. Growth 73 (1985) 316–328.
[6] S.-Z. Lu, A. Hellawell, Metall. Mater. Trans. A 18 (1987) 1721–1733.
[7] M. Shamsuzzoha, L.M. Hogna, Philos. Mag. A 54 (1986) 459–477.
[8] S.-Z. Lu, A. Hellawell, JOM 47 (1995) 38–40.
[9] A. Knuutinen, K. Nogita, S.D. McDonald, A.K. Dahle, J. Light Met. 1 (2001) 229–240.
[10] M. Javidani, D. Larouche, Int. Mater. Rev. 59 (2014) 132–158.
[11] W.J. Kyffin, W.M. Rainforth, H. Jones, J. Mater. Sci. 36 (2001) 2667–2672.
[12] D.H.St. John, L.M. Hogan, J. Aust. Inst. Met. 22 (1977) 160–166.
[13] T. Wang, H. Fu, Z. Chen, J. Xu, J. Zhu, F. Cao, T. Li, J. Alloys Comp. 511 (2012) 45–49.
[14] G.S.V. Kumar, B.S. Murty, M. Chakraborty, J. Alloys Comp. 472 (2009) 112–120.
[15] Y. Birol, J. Alloys Comp. 486 (2009) 219–222.
[16] G.K. Sigworth, M.M. Guzowski, AFS Trans. 93 (1985) 907–912.
[17] T. Sritharan, H. Li, J. Mater. Process. Technol. 63 (1997) 585–589.
[18] J.A. Spittle, J.M. Keeble, A.L. Meshhedani, Light Met. (1997) 795–800.

[19] S.A. Kori, V. Auradi, B.S. Murty, M. Chakraborty, Mater. Forum 29 (2005) 387–393.
[20] P.S. Cooper, A. Hardman, D. Boot, E. Burhop, Light Met. (2003).
[21] M.N. Binney, D.H. St. John, A.K. Dahle, J.A. Taylor, E. Burhop, P.S. Cooper, Light Met. (2003).
[22] M. Nowak, L. Bolzoni, N. Hari Babu, Mater. Des. 66 (2015) 366–375.
[23] L. Bolzoni, M. Nowak, N. Hari Babu, Mater. Des. 66 (2015) 376–383.
[24] L. Bolzoni, M. Nowak, N. Hari Babu, J. Alloys Comp. 623 (2015) 79–82.
[25] M. Nowak, W.K. Yeoh, L. Bolzoni, N. Hari Babu, Mater. Des. 75 (2015) 40–46.
[26] L. Bolzoni, N. Hari Babu, J. Mater. Process. Technol. 222 (2015).
[27] H. Ye, J. Mater. Eng. Perform. 12 (2003) 288–297.
[28] Z. Jeffries, Chem. Met. Eng. 26 (1922) 750–754.
[29] M.D. Hanna, S.-Z. Lu, A. Hellawell, Metall. Trans. A 15 (1984) 459–469.
[30] L. Bolzoni, M. Nowak, N. Hari Babu, Mater. Sci. Eng., A 628 (2015) 230–237.
[31] P. Schumacher, B.J. Mc Kay, J. Non-Cryst. Solids 317 (2003) 123–128.
[32] J.A. Taylor, in: J. Couzner (Ed.), 35th Australian Foundry Institute National Conference, Australian Foundry Institute (AFI), Adelaide, South Australia, 2004, pp. 148–157.